ChemComm

COMMUNICATION

View Article Online
View Journal | View Issue

Cite this: *Chem. Commun.*, 2019, 55, 9697

Received 18th June 2019,
Accepted 18th July 2019

DOI: 10.1039/c9cc04665h

rsc.li/chemcomm

A chiral signal-amplified sensor for enantioselective discrimination of amino acids based on charge transfer-induced SERS†

Yue Wang,[a] Jing Liu,[a] Xueqi Zhao,[a] Chunguang Yang,[a] Yukihiro Ozaki,[b] Zhangrun Xu,*[a] Bing Zhao*[c] and Zhi Yu*[d]

An ultra-high sensitivity sensor with the function of chiral signal amplification has been proposed for the enantiomer discrimination of various amino acid enantiomers based on charge transfer (CT)-induced SERS spectroscopy. The introduced TiO_2 in this sensor improves the CT behavior and discrimination efficiency distinctly and enantiomeric discrimination is realized even at low concentration.

Chiral discrimination has attracted keen interest in various fields, such as chemical and biological sciences and pharmaceutical industries, since life processes are accompanied by chiral selection with a preference for homochiral molecules.[1–3] Amino acids, as one of the molecular building blocks of life, are involved in a vast majority of biological processes in living systems.[4–6] Most amino acids exist in chiral structures, and the two enantiomers exhibit different biological, pharmacological and toxicological activities. Considering the enantioselectivity for L-amino acids in organisms, enantiomeric discrimination of amino acids has aroused considerable attention. The aromatic amino acids are particularly important in many fields, such as metabolism of life, nutriology and pharmacopedics.[7,8] Various techniques have been developed for chiral discrimination;[9–14] however, these methods always require either a specialized chiral entity as a chiral selector or the use of chiral light fields to acquire satisfactory recognition results. There are very few reports on label-free methods for enantiomeric discrimination, like colorimetric methods,[15] and they are vulnerable to environmental interference, considering that the discrimination mainly depends on the aggregation of nanoparticles (NPs). Moreover, high concentration, even for a pure liquid chiral sample, and universality are normally required in some chiral discrimination methods. A simple, generic, and sensitive method for enantiomeric discrimination remains challenging.

Generally, the identification of an amino acid enantiomer is achieved based on the difference in the stereo-structure of a chiral selector and each of the enantiomers, and the discrimination capability mainly depends on the weak intermolecular interactions between the selector molecules and the two enantiomers.[16] Macrocyclic molecules like cyclodextrins (CDs) have been found to be a powerful selector for molecular recognition, since they provide sufficient intermolecular interaction sites and an obvious steric effect to distinguish the enantiomers.[17,18] Considering their special molecular structures composed of hydrophobic internal cavities and hydrophilic external rings, CDs show an advantage of interaction with chiral molecules, especially the ones with hydrophobic groups and suitable molecular size.[18,19] However, despite the introduction of macrocyclic molecules in a discrimination system, a strategy for efficient characterization of the difference of stereostructures caused by two enantiomers of one amino acid with a satisfactory sensitivity remains a key issue for chiral discrimination so far.

Owing to its ultra-high sensitivity and with provision of the enriched structural information, surface-enhanced Raman scattering (SERS) spectroscopy has been developed to be a powerful surface and interface analysis technique not only for exploring the structure, orientation, and adsorption of a molecule but also for trace analysis and detection.[20–22] Since SERS spectroscopy is extremely sensitive to slight changes in molecular electronic structure caused by intermolecular interactions between a probe molecule and its surroundings, it allows for chiral discrimination on the basis of the interaction between probe molecules and surrounding chiral molecules.[23,24] Based on the chiral "label-free" discrimination mechanism we proposed previously,[25,26] we developed a sensor for highly sensitive and efficient enantiomeric recognition in the present work. TiO_2 NPs were introduced in the enantioselective sensor to fabricate Ag–TiO_2–Ag sandwich substrates to improve the charge transfer (CT) behaviour and enlarge the discrimination efficiency, due to their excellent contribution to SERS enhancement

[a] *Department of Chemistry, College of Sciences, Northeastern University, Shenyang 110819, People's Republic of China. E-mail: xuzr@mail.neu.edu.cn*
[b] *Department of Chemistry, School of Science and Technology, Kwansei Gakuin University, Sanda, Hyogo 669-1337, Japan*
[c] *State Key Laboratory of Supramolecular Structure and Materials, Jilin University, Changchun 130012, People's Republic of China. E-mail: zhaob@mail.neu.edu.cn*
[d] *The Guo China-US Photonics Laboratory, Changchun Institute of Optics, Fine Mechanics and Physics, Chinese Academy of Sciences, Changchun, 130033, People's Republic of China. E-mail: zhiyu@chomp.ac.cn*

† Electronic supplementary information (ESI) available. See DOI: 10.1039/c9cc04665h

by the CT mechanism.[27] Chiral difference magnification by *p*-aminothiophenol (PATP), together with stereo selective capture by mono (6-mercapto-6-deoxy)-beta-cyclodextrin (β-CD) in this enantioselective sensor allows the discrimination of enantiomers with low concentration. The excitation wavelength-dependent SERS experiments verified that TiO_2 NPs enhanced photo-induced CT behaviour involved in the discrimination process and enlarged the chiral differences between the two enantiomers.

Herein, we demonstrate the excellent discrimination response to different L-amino acid enantiomers with high sensitivity in comparison to D-amino acids by our enantioselective sensor, especially for the amino acids with appropriate molecular size matching the cavity of β-CD, such as tryptophan (Trp). Even for the amino acids not matching the β-CD very well, including phenylalanine (Phe) and tyrosine (Tyr), the enantioselective sensor also shows satisfactory discrimination sensitivity.

The sandwich Ag–TiO_2–Ag substrate was fabricated by a step-by-step assembly route, and the morphologies are shown in the SEM images in Fig. S1 (ESI†). The average diameters of the Ag NPs and the TiO_2 NPs we used are 60–70 nm and 450 nm, respectively. Considering the excellent CT enhancement of TiO_2 NPs on SERS and the difference of crystal phase structures in enhancement performance,[27–29] a SERS experiment was conducted to investigate the enhancement of Raman scattering for the Ag–TiO_2–Ag substrate with TiO_2 NPs calcined at different temperatures (Fig. S2, ESI†). The Ag–TiO_2–Ag substrate with TiO_2 NPs calcined at 450 °C was proved to possess the optimal SERS signal arising from both electromagnetic (EM) and CT enhancement, and thus was used in the subsequent SERS experiments. With consecutive modification of β-CD and PATP to fabricate the enantioselective sensor as illustrated in Scheme 1, the maximum absorption peak of Ag–TiO_2–Ag substrate redshifted and broadened gradually (Fig. S3, ESI†), due to the changes in the dielectric constant around the Ag NPs on the substrate after it was coated with β-CD and the adjacent PATP molecules.

Upon exposure of the enantioselective sensor to L- and D-Trp solution, the enantioselective sensor demonstrates a pretty good discrimination performance on a Trp solution with the concentration of 10^{-3} M rather than the pure liquid, demonstrating the key role of the CT contribution in the enantiodiscrimination by SERS, aside from the universal EM enhancement resulting from our previous methods (Fig. 1(A)). In consideration of the localized

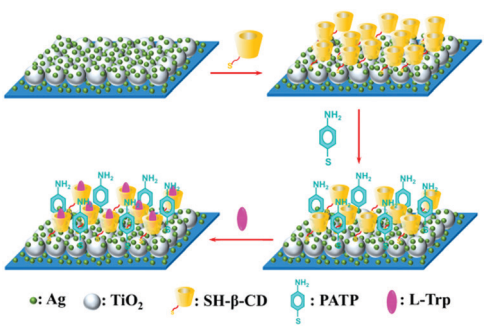

Scheme 1 An illustration of the fabrication processes of the enantioselective sensor, and the enantiodiscrimination of amino acids.

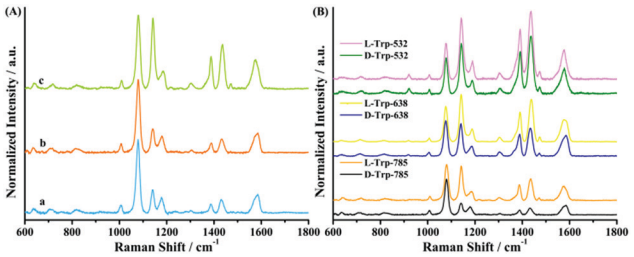

Fig. 1 (A) SERS spectra of PATP modified on the enantioselective sensor in the blank system (a), and the sensor for discriminating D-Trp (b) and L-Trp (c) with the excitation of 785 nm. (B) SERS spectra of PATP in the sensor for discriminating Trp enantiomers with the wavelengths of 532, 638, and 785 nm.

surface plasmons of the substrates,[25] all the SERS spectra acquired were normalized by the PATP band at 1075 cm^{-1} belonging to totally symmetric (a_1) modes, which are insensitive to CT. When L-Trp was introduced in the sensor, the intensities of the non-totally symmetric (b_2) modes of PATP at 1141, 1398, 1435 and 1573 cm^{-1} were obviously enhanced. The increased b_2 modes, which are forbidden in non-resonance conventional Raman spectra, are expected to explain the interactions between molecular π-electrons and the Ag–TiO_2–Ag substrate in the sensor. However, no visible change was observed in the case of the D-Trp sensing system with respect to the blank system without amino acid (Fig. 1(A)b and a), which indicates that L-Trp was selectively recognized by the sensor. Besides Trp, this enantioselective sensor has certain generality and shows favourable discrimination behaviour of Phe and Tyr, which do not match exactly the β-CD (see the SERS spectra in Fig. S4A and B, ESI†).

In addition, visible excitation wavelength-dependent phenomena were obtained from the SERS spectra of PATP in the Trp enantiomer sensing system with excitations at 532, 638, and 785 nm, as shown in Fig. 1(B). The discrepancy of the relative intensities of the b_2 modes of PATP between L- and D-Trp systems decreased with the increase of the laser energy, which manifests that the enantioselective sensor possessed the best discrimination response under the condition of 785 nm laser excitation with the lowest energy. The enantioselective discrimination was closely dependent on the excitation wavelength, indicating that a CT process was involved in this chiral discrimination sensing system and the CT process was influenced by enantioselectivity.[30,31]

The discrimination mechanism closely related with the CT process was proposed by taking Trp as a model with the excitation wavelength of 785 nm. The b_2 modes increased in the presence of L-Trp, but little variation was observed with D-Trp existing in the system (Fig. 1(A)), indicating that the L enantiomer rather than the D enantiomer promoted the CT from the Ag NPs in the Ag–TiO_2–Ag substrate to the PATP. As is known, different intermolecular interactions between the enantiomers result in the stereoselectivity of CD to each enantiomer with a different geometry and stabilization energy. In this enantioselective sensor, the hydrophobic aromatic ring of Trp was drawn in the hydrophobic cavity of β-CD with hydrophobic interactions, while the polar part was excluded outside the mouth of β-CD by forming H-bonds with the hydroxyl group of the CD and the amino group of the PATP, as illustrated in Fig. 2A.

The difference in forming hydrogen bonds led to the enantioselectivity for L-Trp, and thus, influenced the molecular electronic structure of the PATP molecules in the two chiral sensing systems, which caused the difference in the CT process and the evident distinction in the SERS spectra between the two systems. Our previous work demonstrated that the intermolecular H-bond changed the molecular electronic structure, increased the molecular conjugation, and promoted the CT process from metal NPs to the adsorbed molecule in the system.[25] Consequently, a chiral discrimination method based on the intermolecular H-bond of the assembled system by the SERS involving CT mechanism was proposed to identify the chirality of some pure chiral alcohol enantiomers around achiral probe molecules. In the enantiomeric discrimination system, the CT contribution is beneficial to distinguish the discrepancy of the SERS spectra between the two enantiomeric systems, and the key for the enantioselectivity is the subtle difference of the intermolecular interaction in stereostructures between the enantiomers and the sensor. As a result, L-Trp was selectively discriminated by virtue of the promotion of L enantiomers to the CT between the Ag–TiO_2–Ag substrate and the PATP. The PATP in the sensor acted as a magnifier, while the β-CD captured the amino acid enantiomer into its cavity and provided highly sensitive enantioselectivity. If the β-CD was not contained in the enantioselective sensor, poorer discrimination performance was observed from the SERS spectra (Fig. S5, ESI†).

As for the reason why the enantioselective sensor exhibited a superior discrimination response with the 785 nm excitation compared with the other two, an energy level schematic diagram with regards to the corresponding energy levels of Ag, TiO_2, and PATP is illustrated for a better understanding (Fig. 2B).[32] The introduction of TiO_2 promotes electrons congregated at the surface of the TiO_2 to inject into the Fermi level (E_f) of the Ag NPs to balance charges at the junction of the Ag and the TiO_2, which augments the CT from the Ag NPs to the PATP molecules in the enantioselective discrimination sensor.[33] The energy of the three laser excitations is sufficient to excite the electrons from the elevated Fermi level of the Ag NPs to the lowest unoccupied molecular orbital (LUMO) level of the PATP. However, the energy of 785 nm excitation was the lowest and less matched the CT states of PATP compared with the other two excitations. Considering that the CT enhancement for 785 nm is the smallest, it was the most suitable to investigate the promotion of the L-amino acid to the CT in the system at 785 nm excitation. The introduction of the TiO_2 NPs to the enantioselective sensor enhances the CT contribution in the system greatly and results in a superior discrimination performance than the discrimination system without TiO_2 NPs (Fig. S6, ESI†). In the case of the sensor consisting of Ag NPs without TiO_2 NPs, the discrepancy in the relative intensities of the b_2 modes between the L- and D-Trp enantiomeric systems was smaller than the enantioselective sensor containing the TiO_2 NPs (Fig. 1(A)).

In order to obtain the maximum discrimination efficiency and sensitivity, the concentration of adsorbed PATP was optimized. The PATP solutions with different concentrations were investigated by concentration-dependent SERS, and the concentration of 10^{-4} M was chosen for the optimal enantioselective discrimination of the sensor with the 785 nm laser excitation (Fig. S7, ESI†). The sensitivity of the enantiodiscrimination method was investigated subsequently by measuring the SERS spectra of the discrimination sensing system with different concentrations of L- and D-Trp enantiomers (Fig. 3) under the optimized conditions. A positive correlation was observed between the SERS intensity of the b_2 modes of PATP and the amount of L-Trp enantiomer; however, no obvious relevance was obtained when the D-Trp enantiomer was involved in the system. The higher the concentration of L-Trp the greater the enhancement of the b_2 modes of PATP, which led to a larger intensity difference between the L- and D-Trp sensing systems and a much easier identification of the two enantiomers.

We calculated the degree of CT (ρ_{CT}), an expression to estimate the contribution of CT to the Raman enhancement in a SERS system proposed by Lombardi *etc.*,[34,35] to evaluate the discrimination capacity of the sensor between D and L enantiomers of Trp (see ESI† for the details). Fig. 4 reveals that the magnitude of the difference of the ρ_{CT} between D- and L-Trp increases with the concentration of Trp molecules, which was consistent with the obtained SERS spectra in Fig. 3. The minimum enantiomeric discrimination concentration for L-Trp is 0.1 μmol L^{-1}, which is much lower than the minimum level of L-Trp in the human serum. Even for Phe, which does not match with β-CD well, the minimum discrimination concentration for L-Phe is 1 μmol L^{-1} (Fig. S8, ESI†), which is also

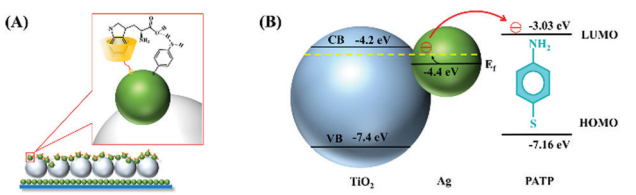

Fig. 2 (A) A schematic illustration of the interactions of SH-β-CD and PATP on the sensor with L-Trp enantiomers in the discrimination process. (B) An energy level diagram of the Ag NP, TiO_2 NP and PATP.

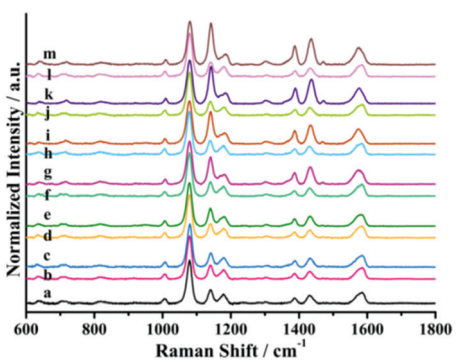

Fig. 3 SERS spectra of PATP in the enantioselective sensor for discriminating D- and L-Trp enantiomers with different concentrations with the excitation of 785 nm; spectrum a is the blank one without Trp, and spectra b to m represent D- and L-Trp enantiomers with concentrations of 10^{-8}, 10^{-7}, 10^{-6}, 10^{-5}, 10^{-4}, and 10^{-3} mol L^{-1}, respectively.

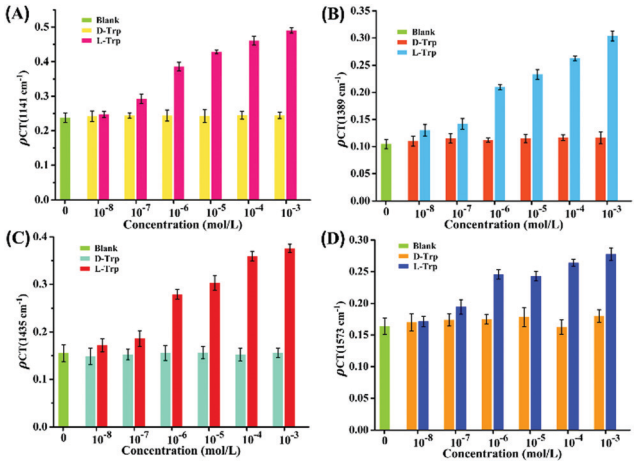

Fig. 4 Degree of CT (ρ_{CT}) for PATP *versus* the concentration of Trp in the enantiodiscrimination sensing system, including the bands at 1141 (A), 1389 (B), and 1435 (C), and 1573 (D) cm^{-1} in Fig. 3.

much lower than the minimum level in human serum. The enantiomeric discrimination approach proposed by us exhibits a high sensitivity and discrimination efficiency.

In conclusion, we have developed an enantioselective sensor for the discrimination of various amino acid enantiomers. Due to the intermolecular interaction, mainly the hydrogen-bond, between the amino acid enantiomers and the sensing unit consisting of β-CD and PATP, the sensor can distinguish and magnify the subtle changes of weak interactions caused by the stereoselectivity in the SERS spectra with the contribution of the CT mechanism. PATP acted as a magnifier to amplify the difference in the intermolecular interactions between the two enantiomers and the sensor, while β-CD captured the amino acid enantiomer into its cavity and provided quite sensitive enantioselectivity in the enantioselective sensor. The suggested mechanism is that differentiable CT processes are involved in the two enantioselective sensing systems, leading to the difference in molecular electronic structure of the PATP and the selectively enhanced b_2 modes of the PATP with L-enantiomer introduced in the sensor based on the excitation wavelength dependent SERS results. The enantioselective sensor shows a pretty good discrimination performance for trace amino acid aqueous solutions with ultrahigh-sensitivity, simplicity and universality. We have provided a distinctive way to implement enantiomeric discrimination of amino acid aqueous solutions with simplicity and high enantioselectivity, which has great potential for wide application to various chiral samples in the fields of biochemistry, asymmetric synthesis, and the pharmaceutical industry.

We are grateful for the financial support from NSFC (Grant No. 21705015, 21675020, 61705227, 21773080, and 21711540292) of P. R. China; the Fundamental Research Funds for the Central Universities (N170504013); and the Open Project of State Key Laboratory of Supramolecular Structure and Materials (Grant No. SKLSSM201824).

Conflicts of interest

There are no conflicts to declare.

Notes and references

1 F. Zhang, C. Lu, M. Wang, X. Yu, W. Wei and Z. Xia, *ACS Sens.*, 2018, **3**, 304–312.
2 J. Y. C. Lim, I. Marques, V. Felix and P. D. Beer, *Angew. Chem., Int. Ed.*, 2018, **57**, 584–588.
3 H. E. Lee, H. Y. Ahn, J. Mun, Y. Y. Lee, M. Kim, N. H. Cho, K. Chang, W. S. Kim, J. Rho and K. T. Nam, *Nature*, 2018, **556**, 360–365.
4 G. Fukuhara and Y. Inoue, *Chem. – Eur. J.*, 2012, **18**, 11459–11464.
5 L. Zhang, G. Wang, C. Xiong, L. Zheng, J. He, Y. Ding, H. Lu, G. Zhang, K. Cho and L. Qiu, *Biosens. Bioelectron.*, 2018, **105**, 121–128.
6 M. M. Wanderley, C. Wang, C. D. Wu and W. Lin, *J. Am. Chem. Soc.*, 2012, **134**, 9050–9053.
7 D. Dodd, M. H. Spitzer, W. V. Treuren, B. D. Merrill, A. J. Hryckowian, S. K. Higginbottom, A. Le, T. M. Cowan, G. P. Nolan, M. A. Fischbach and J. L. Sonnenburg, *Nature*, 2017, **551**, 648–652.
8 T. J. Ritchie, S. J. F. Macdonald, R. J. Young and S. D. Pickett, *Drug Discovery Today*, 2011, **16**, 164–171.
9 M. M. K. Sharaf El-Din, K. A. M. Attia, M. W. I. Nassar and M. M. Y. Kaddah, *Talanta*, 2018, **189**, 86–91.
10 T. Noguchi, B. Roy, D. Yoshihara, J. Sakamoto, T. Yamamoto and S. Shinkai, *Angew. Chem., Int. Ed.*, 2017, **56**, 12518–12522.
11 M. Pushina, S. Farshbaf, E. G. Shcherbakova and P. Anzenbacher, *Chem. Commun.*, 2019, **55**, 4495–4498.
12 M. G. Lizio, V. Andrushchenko, S. J. Pike, A. D. Peters, G. F. S. Whitehead, I. J. Vitorica-Yrezabal, S. T. Mutter, J. Clayden, P. Bour, E. W. Blanch and S. J. Webb, *Chem. – Eur. J.*, 2018, **24**, 9399–9408.
13 H. Su, Q. Zheng and H. Li, *J. Mater. Chem.*, 2012, **22**, 6546–6548.
14 Y. Tang and A. E. Cohen, *Science*, 2011, **332**, 333–336.
15 L. Zhang, C. Xu, C. Liu and B. Li, *Anal. Chim. Acta*, 2014, **809**, 123–127.
16 L. You, D. Zha and E. V. Anslyn, *Chem. Rev.*, 2015, **115**, 7840–7892.
17 H. Y. Ching, S. Clifford, M. Bhadbhade, R. J. Clarke and L. M. Rendina, *Chem. – Eur. J.*, 2012, **18**, 14413–14425.
18 J. Yang, Y. Yu, D. Wu, Y. Tao, L. Deng and Y. Kong, *Anal. Chem.*, 2018, **90**, 9551–9558.
19 G. Xie, W. Tian, L. Wen, K. Xiao, Z. Zhang, Q. Liu, G. Hou, P. Li, Y. Tiana and L. Jianga, *Chem. Commun.*, 2014, **51**, 3135–3138.
20 S. Ding, J. Yi, J. Li, B. Ren, D. Wu, R. Panneerselvam and Z. Tian, *Nat. Rev. Mater.*, 2016, **1**, 16021.
21 S. Schlucker, *Angew. Chem., Int. Ed.*, 2014, **53**, 4756–4795.
22 S. Laing, K. Gracie and K. Faulds, *Chem. Soc. Rev.*, 2016, **45**, 1901–1918.
23 Y. Wang, W. Ji, H. Sui, Y. Kitahama, W. Ruan, Y. Ozaki and B. Zhao, *J. Phys. Chem. C*, 2014, **118**, 10191–10197.
24 Y. Wang, W. Ji, Z. Yu, R. Li, X. Wang, W. Song, W. Ruan, B. Zhao and Y. Ozaki, *Phys. Chem. Chem. Phys.*, 2014, **16**, 3153–3161.
25 Y. Wang, Z. Yu, W. Ji, Y. Tanaka, H. Sui, B. Zhao and Y. Ozaki, *Angew. Chem., Int. Ed.*, 2014, **53**, 13866–13870.
26 Y. Wang, Z. Yu, X. Han, H. Su, W. Ji, Q. Cong, B. Zhao and Y. Ozaki, *J. Phys. Chem. C*, 2016, **120**, 29374–29381.
27 L. Yang, X. Jiang, W. Ruan, B. Zhao, W. Xu and J. R. Lombardi, *J. Phys. Chem. C*, 2008, **112**, 20095–20098.
28 X. X. Han, W. Ji, B. Zhao and Y. Ozaki, *Nanoscale*, 2017, **9**, 4847–4861.
29 Y. Wang, J. Liu, Y. Ozaki, Z. Xu and B. Zhao, *Angew. Chem., Int. Ed.*, 2019, **58**, 8172–8176.
30 Z. Mao, W. Song, X. Xue, W. Ji, Z. Li, L. Chen, H. Mao, H. Lv, X. Wang, J. R. Lombardi and B. Zhao, *J. Phys. Chem. C*, 2012, **116**, 14701–14710.
31 W. Ji, Y. Kitahama, X. Xue, B. Zhao and Y. Ozaki, *J. Phys. Chem. C*, 2012, **116**, 2515–2520.
32 Z. Sun, C. Wang, J. Yang, B. Zhao and J. R. Lombardi, *J. Phys. Chem. C*, 2008, **112**, 6093–6098.
33 L. Yang, W. Ruan, X. Jiang, B. Zhao, W. Xu and J. R. Lombardi, *J. Phys. Chem. C*, 2009, **113**, 117–120.
34 J. R. Lombardi and R. L. Birke, *J. Phys. Chem. C*, 2008, **112**, 5605–5617.
35 J. R. Lombardi, R. L. Birke, T. Lu and J. Xu, *J. Chem. Phys.*, 1986, **84**, 4174–4180.

